

# Simulation of Progressive Damage Development in Braided Composite Tubes Undergoing Dynamic Axial Crushing

Carla McGregor<sup>a</sup>, Reza Vaziri<sup>a</sup>, Anoush Poursartip<sup>a</sup>, Xinran Xiao<sup>b</sup>, Nancy Johnson<sup>b</sup>

<sup>a</sup>*Composites Group, Departments of Civil Engineering and Materials Engineering, The University of British Columbia, Vancouver, British Columbia, Canada, V6T 1Z4*

<sup>b</sup>*General Motors Corporation, Research & Development, MC 480-106-710, 30500 Mound Road, Warren, MI 48090-9055*

## Abstract

*Composite tubular structures are of interest as viable energy absorbing components in vehicular front rail structures to improve crashworthiness. Desirable tools in designing such structures are models capable of simulating damage growth in composite materials. CODAM (COmposite DAMage), which is incorporated into LS-DYNA as a user material model, is a continuum damage mechanics based model for composite materials with physically based input parameters. In this paper, the CODAM model is used to simulate tube crush experiments. It is shown that the damage propagation, fracture morphology and energy absorption predictions correlate well with the experimental results.*

## Introduction

An extensive body of literature indicates that stable progressive crushing and high specific energy absorption (SEA) is attainable in fibre reinforced composite tubular structures. Energy is absorbed through a complex combination of numerous fracture mechanisms. The actual fracture behaviour is dependent on the material parameters (fibre and matrix type [1-8], fibre architecture [2-4,7,9-11], and fibre volume fraction [12]), specimen geometry [13-17], and external loading conditions [5,18-23].

Accurate numerical tools, capable of predicting the crushing behaviour and energy absorption trends in these structures would reduce the time and costs associated with testing and potentially provide a useful design aid. However, predicting the response is a difficult task due to the complex nature of the damage and fracture mechanisms and the lack of accurate and robust predictive numerical tools. There have been a number of attempts to simulate the crushing response of composite tubes using finite element analysis (FEA) in conjunction with a constitutive model that simulates damage initiation, damage growth and final fracture. Typically, either a micromechanical or a macromechanical approach is adopted.

Micromechanical approaches represent damage growth at the level of the constituents and use this information in the global model to define the overall response of the laminate at any level of loading. Although potentially very accurate, these models tend to be fairly complex and inefficient when attempting to model full scale dynamic tube crushing events. Beard and Chang [24] used a micromechanical model incorporated into the ABAQUS implicit code to simulate the complete crushing process of triaxially braided composite tubes with promising initial results. The material model is yet to be implemented into explicit codes for dynamic analysis of crash events.

Macromechanical (or phenomenological) approaches represent the effect of damage growth in the individual constituents by smearing the response over a Representative Volume of Element

(RVE). There is a trade off between the accuracy and robustness provided by micromechanical models and the efficiency and flexibility provided by macromechanical models. Most macromechanical schemes approach the problem by defining damage and fracture criteria, which once exceeded, leads to either a reduction in the elemental stiffness and strength properties (as was done by Kerth and Maier [25]) or the complete removal of the element representing the particular ply (as was done by Caliskan [26]). These models, although simple, still face the challenge of defining the post-peak behaviour in a phenomenological manner. Morthorst and Horst [27] noted that their material model was computationally intensive, requiring numerous parameters, most of which were determined using curve fitting methods. Additionally, these types of strain softening or ply-by-ply failure models tend to result in mesh sensitive results. Xiao et al. [28] presented the results of a study done on braided composite tube crushing simulations using the built-in macromechanical material model, MAT58, in LS-DYNA. The SEA and peak forces in braided tubes crushed with a plug initiator were captured well, but the SEA of non-initiated tube crushes tended to be under-predicted. Although the results were promising, there were some issues regarding the physical nature of the model parameters.

The lack of numerical models capable of truly and efficiently capturing the crushing response of composite tubular structures with physically based model parameters prompted an investigation into the effectiveness of CODAM [29-31], a physics-based macromechanical constitutive model, at predicting the behaviour of these structures. This constitutive model has been implemented as a user material model in the general purpose, explicit non-linear finite element analysis code, LS-DYNA. The main objective was to simulate the damage propagation and specific energy absorption (SEA) in braided composite tubes subjected to axial compression. A supplementary goal was to study the sensitivity of the tube crushing analysis to variations in the model parameters to provide a certain measure of the stability of the simulations and also to offer some insight into methods of improving the SEA of these composite tubes.

### Experimental Details

Results from an experimental tube crushing program conducted in a drop tower facility at General Motors Corporation [22,23] on braided composite tubes [3,4] were used to evaluate the accuracy of our model. The braided composite tubes were made of one, two or four layers of a [0/±30] braid of Fortafil #556 80k carbon fibre tows in an Hetron 922 resin (an epoxy vinyl ester). The quality of the material was generally fair to poor, with warped surfaces, resin-rich regions, poor tow distribution/alignment, and dry and poorly bonded tows.

The tubes were approximately 360 mm in length and had nominal outside dimensions of 55x55 mm. The leading edges of all the tubes were chamfered at a 45° angle. In tubes tested with an additional external initiator, a metal plug was inserted into the bottom of the tube. The specimens were dropped from a height of 2.54 m, resulting in an impact velocity of about 7.1 m/s and impact energy of approximately 3.5 kJ.

The tubes split into very indistinct fronds with tearing concentrated at the corners. Transverse tensile fracture was observed between and within the tows. Away from the corners, the main damage mechanism was observed to be delamination (in multiply lay-ups) followed by bending of the separated material either inwards or outwards.

## Constitutive Model Details

CODAM was used to simulate damage propagation in the braided composite tubes. The model represents the constitutive behaviour through both the elastic (pre-peak) and post-peak regimes. The mechanical consequences of matrix cracking, fibre breakage, and delamination (main fracture mechanisms in tension), and kinking and kink band broadening, in conjunction with matrix cracking and delamination (main fracture mechanisms in compression), are represented in the model.

The model characterizes damage growth in a Representative Volume Element (RVE), defined by dimensions that have physical meaning (Figure 1). The height and width are equal to the characteristic height of damage, defined as the actual height the damage would grow to in a quasi-brittle material if experimentally tested under conditions that lead to stable damage growth. The thickness corresponds to the thickness of the laminate.

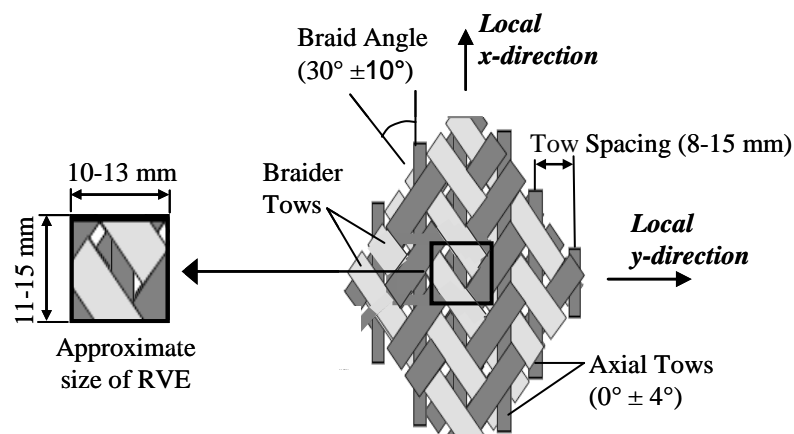


Figure 1 Schematic showing the approximate size of the Representative Volume Element (RVE) for the braided material. Also shown are some dimensional variations in the tow spacing and alignment reported for the material by DeTeresa *et al.* [32].

All parameters defining the material response are defined at the scale of the RVE. They can be segregated into five main categories.

- 1) **Standard Material Properties:** The elastic modulus, shear modulus, and Poisson's ratio in all local directions need to be defined.
- 2) **Progressive Damage Development:** The overall damage state of the RVE is indicated by 3 damage parameters ( $\omega_x$ ,  $\omega_y$ , and  $\omega_z$ ). These parameters are in turn dependent on the strain state of the RVE. To prevent self-healing of the material, the damage parameters are non-decreasing functions that range from 0 (indicating no damage) to 1 (indicating complete damage).
- 3) **Progressive Material Degradation:** As damage within the RVE progresses, the relevant moduli decrease. In CODAM, this is represented by a progressive degradation of the RVE normalized elastic moduli, from 1 (indicating no damage) to 0 (indicating complete fracture).
- 4) **Plateau Stress:** The plateau stress is defined in the compressive domain of each local direction. It arises from the continued ability of the bulk damaged material to support compressive load even though the material is completely damaged. Sivashanker

estimated the plateau stress values to be between 120 to 200 MPa in carbon fibre/epoxy composites [33,34].

- 5) **Scaling Parameters:** Strain-softening material models, such as CODAM, are susceptible to mesh sensitivity [35], which is the tendency of a finite element analysis to produce significantly different results for different mesh densities. A scaling law incorporated into CODAM accounts for element sizes that are different from the RVE size. This scaling law is based on the notion that the fracture energy,  $G_f$ , associated with fracture of a given element with height,  $h_e$ , should be equivalent to the corresponding fracture energy associated with fracture in the same loading direction of the characteristic RVE element with height,  $h_{RVE}$ . In general, the process involves scaling the post-peak stress-effective strain curve in such a way as to maintain the fracture energy constant, i.e.

$$G_f = \gamma_{RVE} \cdot h_{RVE} = \gamma_e \cdot h_e \tag{1}$$

where  $\gamma$  is the fracture energy density, and subscripts  $RVE$  and  $e$  refer to Representative Volume Element and arbitrary finite element, respectively. More detailed explanation of the theory and process used to scale the elemental response in tension and compression can be found in [31,36,37].

The one-dimensional stress-effective strain response of the braided RVE can be constructed using the aforementioned parameters (as shown in Figure 2 for the local x-direction of the braided material aligned with the compressive loading direction). The overall response is characterized by a continual softening (via modulus reduction) as the strain within the RVE increases.

Table 1 summarizes the CODAM parameters that define the complete in-plane orthotropic response of the braided material. These parameters were estimated using information recorded from coupon tests [32], constituent properties and braid architecture. The large variation in the quality and measured material properties of the coupon specimens warranted the use of upper and lower bound parameters.

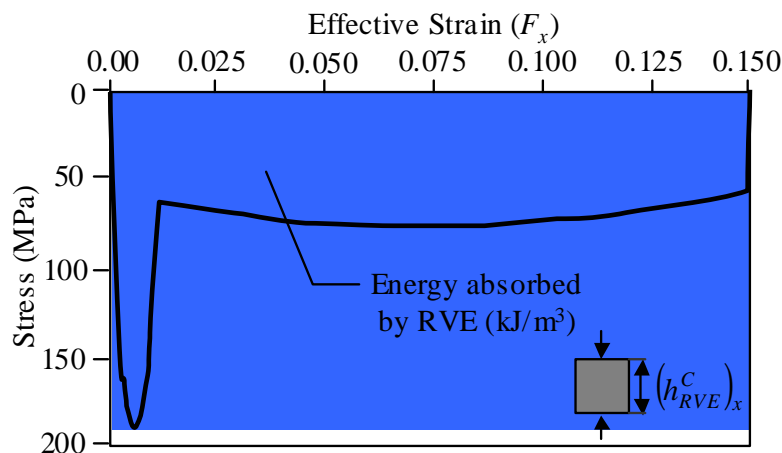


Figure 2 Resulting local x-direction stress vs. effective strain relationship under compressive load for the RVE assuming monotonic loading to fracture.

Table 1

CODAM parameters for  $[0/\pm 30]_n$  braided laminate of Fortafil #556 80k carbon fibre tows in a Hetron 922 resin (an epoxy vinyl ester). Parameters are independent of the number of plies within the laminate.

CODAM Parameters	Local x-direction		Local y-direction	
	Tension	Compression	Tension	Compression
Initial elastic modulus $E^o$ (GPa)	33 - 50	33 - 50	5.7 - 8	5.7 - 8
Matrix damage initiation $F_{mi}^C, F_{mi}^T$	0.006 - 0.008	0.002 - 0.003	0.006 - 0.008	0.006 - 0.008
Matrix damage saturation $F_{ms}^C, F_{ms}^T$	0.021 - 0.025	0.010 - 0.011	0.021 - 0.025	0.021 - 0.025
Fibre damage initiation $F_{fi}^C, F_{fi}^T$	0.006 - 0.008	0.002 - 0.003	0.011 - 0.012	0.007 - 0.009
Fibre damage saturation $F_{fs}^C, F_{fs}^T$	0.021 - 0.025	0.12 - 0.15	0.050 - 0.060	0.120 - 0.150
Damage due to matrix damage saturation $\omega_{ms}$	0.55	0.55	0.55	0.55
Normalized modulus at matrix damage saturation $\bar{E}_{ms}^C, \bar{E}_{ms}^T$	0.87	0.01	0.48	0.02
Plateau stress $\sigma_{plat}$ (MPa)	-	55 - 60	-	45 - 50
Damage height $h_{RVE}^C, h_{RVE}^T$ (mm)	12 - 15	11 - 14	10 - 13	9 - 12
Fracture energy $G_f^C, G_f^T$ (kJ/m <sup>2</sup> )	36 - 101	7.3 - 20	16 - 42	5 - 13

### Finite Element Model

The simulations consisted of 3 main components: a drop weight, a tube and either a plug initiator or a rigid plate as shown in Figure 3. The drop weight was modelled using solid elements as a rigid body with a mass equal to that used in the experiments (140 kg). An initial velocity of 7.1 m/s was assigned to the drop weight causing the tube to impact the plug (or in case of simulation without the plug initiator, the rigid plate). The plug initiator was modelled using solid elements as a rigid body and was fixed in space. The tube was modelled using shell elements and was rigidly attached to the bottom of the drop weight. The composite material for the tube was characterized using CODAM. The local x-direction is aligned with the longitudinal axis of the tube and the local y-direction is aligned at right angles to this axis as shown in Figure 3. Both lower and upper bound CODAM parameters (Table 1) were used in the tube simulations to create bounds on the simulation results.

Under-integrated shell elements, which dramatically reduce the computational run time (by up to 70%), were used in most of the simulations. To prevent non-physical, zero-energy deformation modes, stiffness based hourglass (HG) control was applied.

The option to erode elements, thus removing them completely from the analysis, is included in CODAM. Erosion is helpful when a strain softening material model is defined because degraded elements can distort easily, leading to high hourglass energy. In all the simulations, erosion was based on a total strain criterion, which removes the element once the sum of all the strain components reaches or surpasses a critical limit, defined as

$$|\epsilon_x| + |\epsilon_y| + |\epsilon_z| + |\epsilon_{xy}| + |\epsilon_{yz}| + |\epsilon_{xz}| \geq \text{Erode} \quad (2)$$

In the tube simulations, Erode was set to a high value (ranging from 200 to 300%), ensuring that the element is completely damaged upon removal.

Contact between the tube and the plug (or rigid wall), as well as self-contact of the tube, was modelled using Automatic Single Surface contact type (type 13) due to its reliability and accuracy in crash analyses.

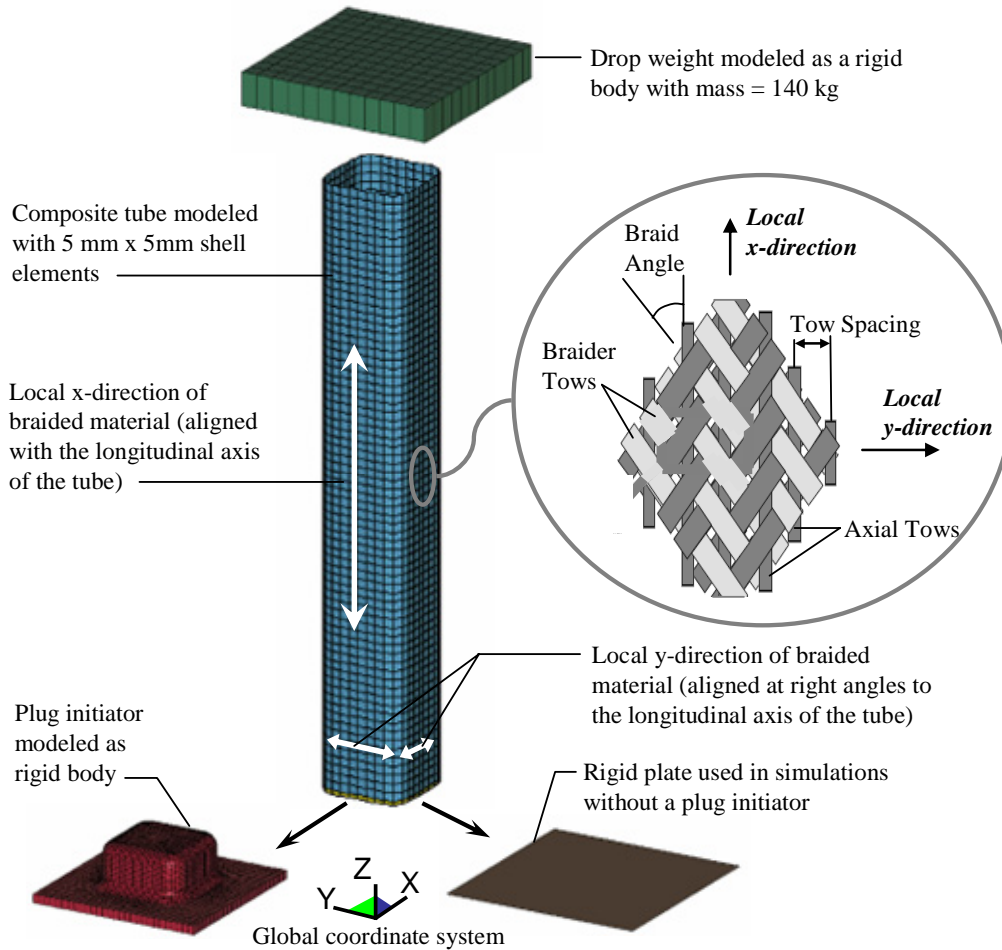


Figure 3 Schematic of the basic components in the tube crushing simulation showing the 2-dimensional braid architecture. The tube contacts either the plug or the rigid plate.

### Simulation Results and Discussion

The success of the numerical model at capturing the observed tube crushing response was based on the comparisons of the force-displacement profile, peak force, overall damage and fracture behaviour and final predicted Specific Energy Absorption (SEA). The energy development was numerically monitored in LS-DYNA using many global and material based energy outputs. Time histories of various forms of energy (kinetic energy, strain energy, total energy) were monitored as a consistency check on energy calculations.

### With Plug

In cases that included an external plug initiator, the tube progressively failed under the applied velocity and split into four fronds, agreeing well with the observed behaviour, as seen in Figure 4. Damage was introduced at the bottom of the tube via high longitudinal stresses that developed due to the 45° chamfer and high circumferential stresses that developed due to the expansion of the tube as it was forced over the plug initiator. After the initial formation, the damage zone progressively advanced up the length of the tube in a self-similar manner. Figure 5 shows the slight localization of the longitudinal and circumferential strains at the corners near the beginning of the simulation. These strains eventually lead to complete fracture of the corner elements. Figure 6 represents the general characteristics of the strain distribution at any given cross-section, given damage has formed and is in the process of self-similar growth.

The predicted upper and lower bound force-displacement profiles are compared to the experimental profile in Figure 7. Aside from the higher number of peaks in the numerical response, the profiles match fairly well; peak force values and average crushing force levels straddle the experimental results. The profiles of various forms of energy recorded by LS-DYNA are shown for the lower bound simulation in Figure 8(a). The total energy in the system remained relatively constant, as the kinetic energy decreased and the internal and frictional energy increased. Figure 8(b) shows various forms of energy absorption in the system. The sliding energy is the energy absorbed at the contact interface via friction. The material internal energy is the energy absorbed by the composite tube, but instantaneously subtracts the energy absorbed by any elements that have eroded. The global internal energy represents the energy absorbed by the composite tube, including the energy absorbed by any elements that have eroded. The energy indicated by the integral of the force-displacement profile, which represents the total energy absorbed by the system, is also shown in the figure. The sum of the global internal energy and the sliding energy approximately equals the energy indicated by the force-displacement profile. In all simulations, approximately 30% of the total energy was absorbed via friction and 70% was absorbed via material straining and damage growth.

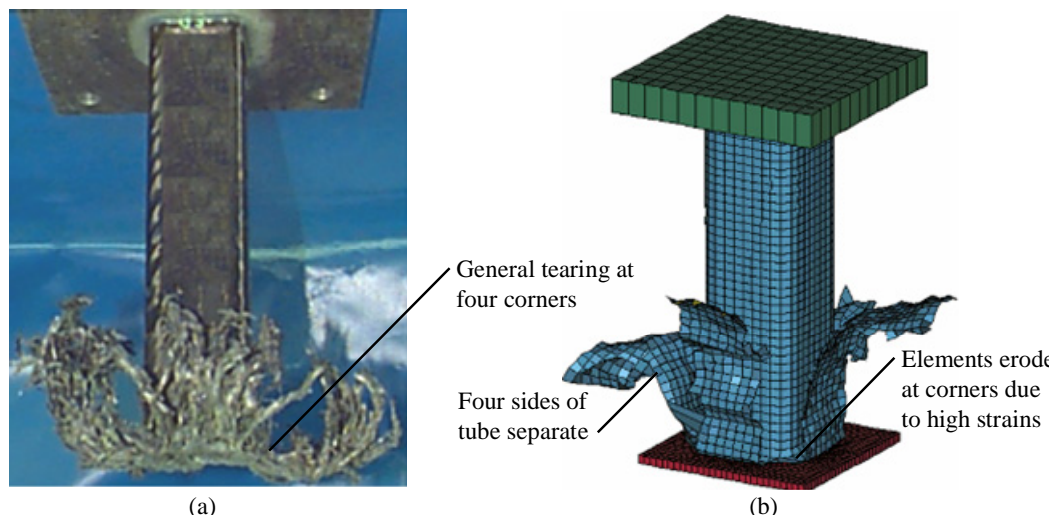


Figure 4 Comparison of (a) experimental [38] and (b) predicted damage and fracture morphology. Both are characterized by general tearing at the four corners.

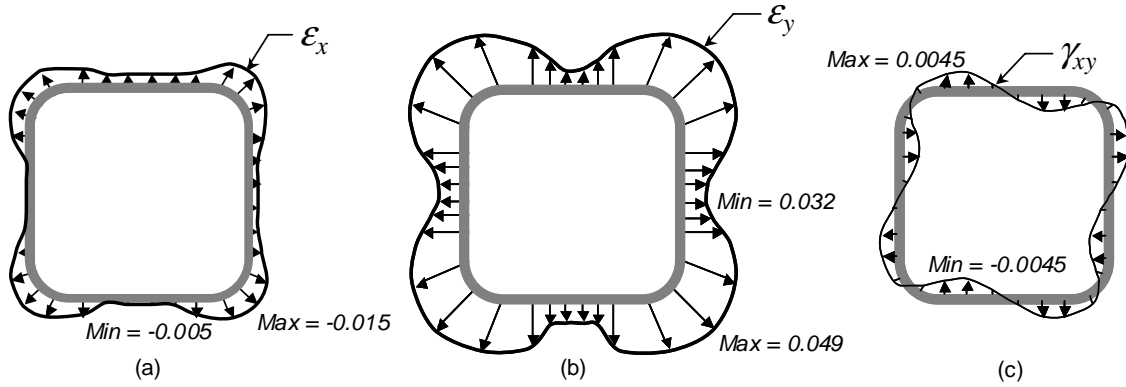


Figure 5 Variation of (a) longitudinal (b) circumferential and (c) in-plane shear strains at the bottom of the tube at an applied longitudinal displacement of 7 mm (Not to scale).

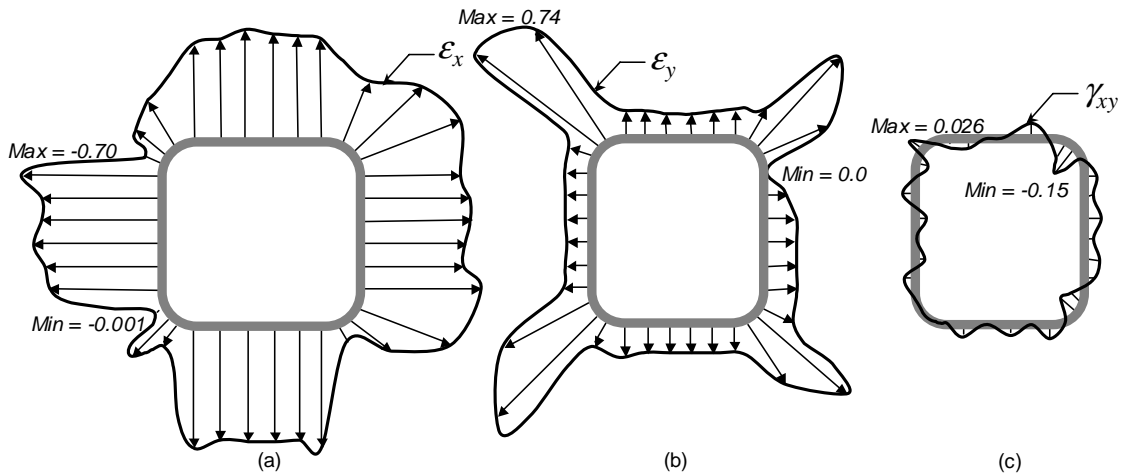


Figure 6 Variation of (a) longitudinal (b) circumferential and (c) in-plane shear strains at the active damaging cross section of the tube at an applied longitudinal displacement of 165 mm (Not to scale).

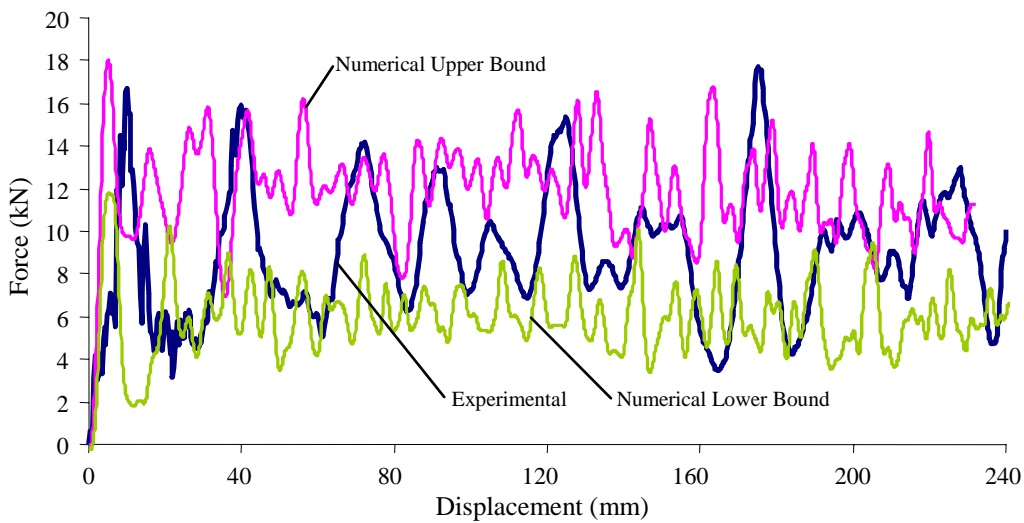


Figure 7 Comparison of predicted upper and lower bound force-displacement profiles to the experimentally measured trace for single ply tube with plug.

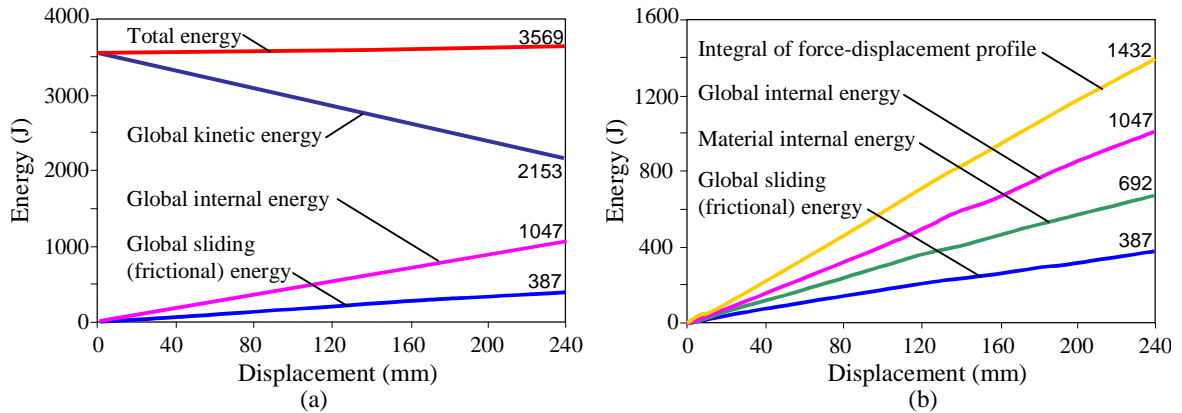


Figure 8 Growth and decay of various (a) global and (b) dissipative energy measures predicted by LS-DYNA as the tube crushes (lower bound parameters).

**Without Plug**

Tubes were also tested without an external plug initiator. They too progressively crushed under the applied velocity and typically resulted in higher energy absorption values. The crushing morphology was slightly less structured, with the formation of very indistinct fronds. The simulation was able to capture the features of this type of damage and fracture quite well, as shown in

Figure 9.

The predicted upper bound force-displacement profile is compared to the experimental profile in Figure 10 (note that the lower bound prediction, which is not included for aesthetic reasons, has a peak force value and average crushing force of about 34 kN and 10 kN). Aside from the higher number of peaks in the numerical response, the profile matches well with peak force values and average crushing force levels being within 10% of the experimental results.

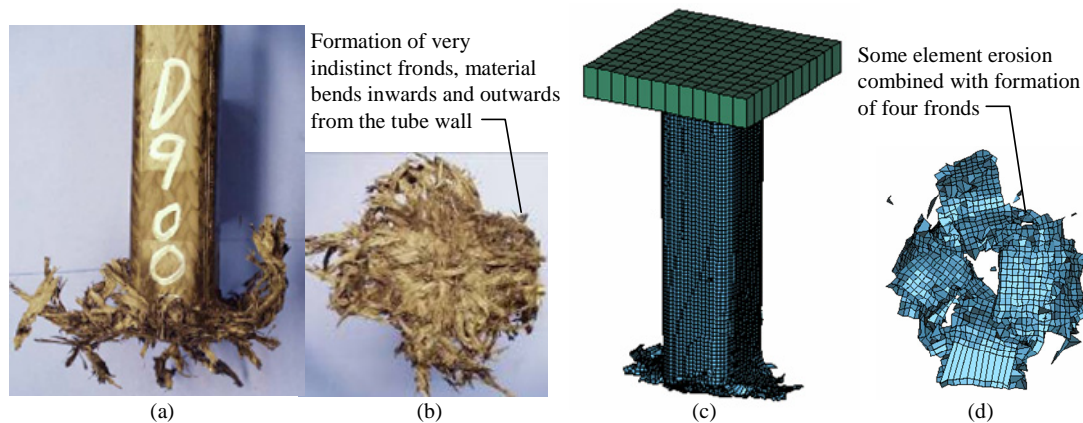


Figure 9 Comparison of (a,b) experimental [32] and (c,d) predicted fracture morphology for tubes crushed without an external plug initiator. Both are characterized by general tearing at the four corners and bending of the damaged material.

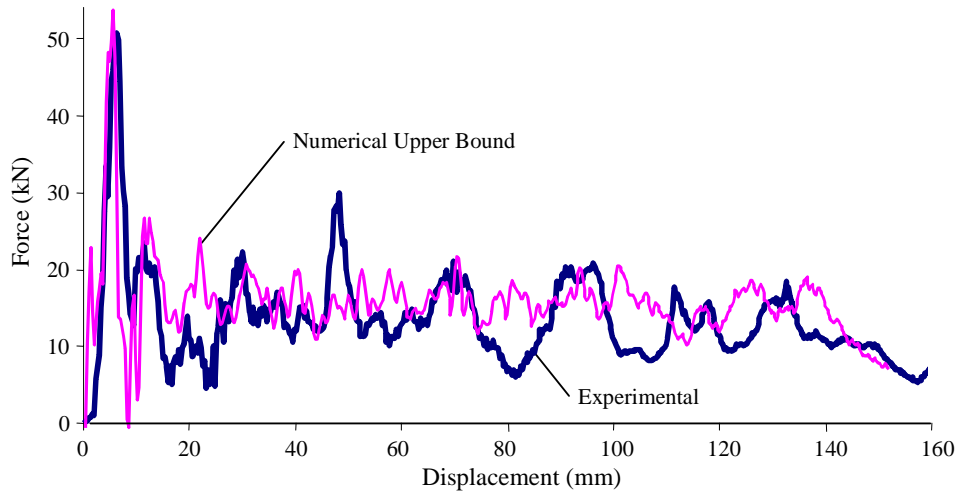


Figure 10 Comparison of predicted upper bound force-displacement profile to the experimentally measured trace for single ply tube without plug.

### Specific Energy Absorption

The effectiveness of composite tubes as energy absorbers in crashworthy structures is most often indicated by the Specific Energy Absorption (SEA). The SEA is defined as the energy absorbed per unit mass of material damaged in the process (Equation 3). In the experimental study, the energy absorbed during crushing was taken as the area under the force-displacement curve and the mass of the crushed portion of the tube was determined using the total mass of the tube and the crushing length, as shown in Equations 4, and 5.

$$SEA = \frac{\text{Energy Absorbed}}{\text{Mass of damaged material}} \quad (3)$$

$$\text{Energy Absorbed} = \int_0^{\delta_f} F d\delta \quad (4)$$

$$\text{Mass of damaged material} = \frac{\text{Crushed length}}{\text{Total length}} (\text{Total mass of tube}) \quad (5)$$

Figure 11 shows the overall comparison between the experimental and numerically predicted peak force and SEA values for all of the tubes studied. The figure presents some key features. The peak force and SEA values increase with increasing wall thickness and as moving from plug initiated to non-plug initiated tests. The simulations were able to pick up these general trends and straddled the experimental results quite well. The limited number of experimental results did not provide much insight into the accuracy of the relatively large bounds predicted by the simulations.

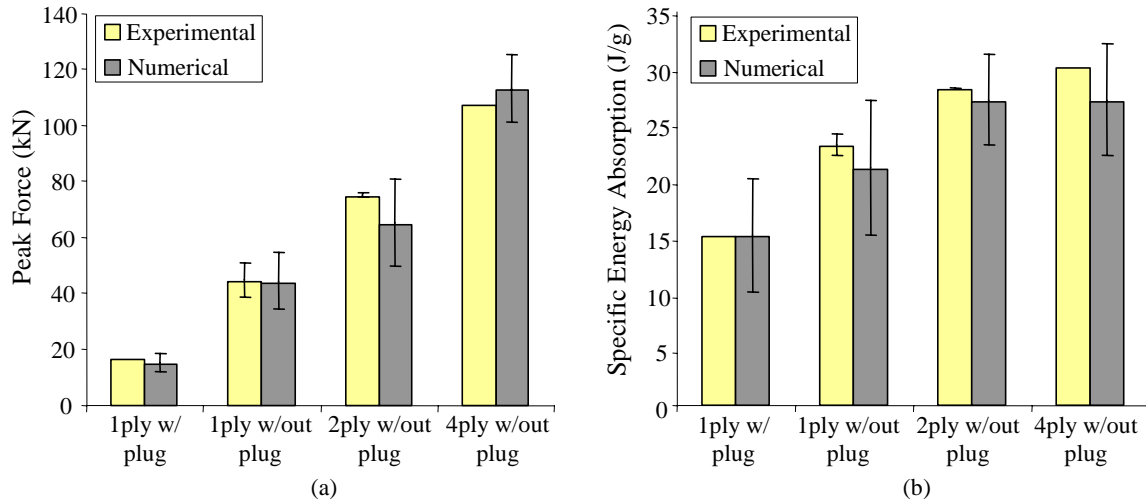


Figure 11 Comparison of measured and predicted (a) peak force and (b) SEA values for single ply, double ply and four ply tubes. Error bars represents the upper and lower bound measurements (experimental) or bounds (numerical).

## Summary and Conclusions

In this paper, a previously developed continuum damage mechanics based model (CODAM), was used to simulate the damage propagation and energy absorption in the axial crushing of braided composite tubes. The inputs to the model are the Representative Volume Element dimensions, the initial elastic moduli of the RVE, the effective strain constants, the effective strain versus damage relationships, and the damage versus normalized moduli relationships. Using these inputs, which were based as much as possible on the physics of damage evolution in the braided composites, the damage propagation, force-displacement profile, and specific energy absorption trends were captured reasonably well.

In plug-initiated tubes the dominant global damage and fracture mechanisms were tearing at the corners due to high circumferential strains, combined with moderate longitudinal compressive damage along the entire perimeter. In tubes simulated without a plug, the dominant global damage and fracture mechanisms were mild tearing at the corners, combined with significant longitudinal compressive damage along the entire perimeter.

The success of the current study suggests that CODAM could offer an attractive design aid for future incorporation of lightweight composite energy absorbers into crashworthy structures. Additionally, this study improves the confidence of using CODAM as a predictive tool to simulate the effect of damage in composites subjected to either tensile or compressive loads.

## Acknowledgements

The financial support for this project provided by the Natural Sciences and Engineering Research Council (NSERC) of Canada and General Motors of Canada through a Collaborative Research and Development grant is greatly appreciated

## References

1. Browne, Alan L., and Johnson, Nancy L., "Dynamic Axial Crush Tests of Roll Wrapped Tubes: Tube Geometry and Material Effects," presented at the ASC 20th Annual Technical Conference, 9/08/05, Drexel University, Philadelphia PA., and published as paper No. 2 in the Conference CD "*Proceedings of the Joint American Society for Composites*", Sept. 2005.
2. Browne, A. L., Iobst, S., "Dynamic Axial Crush of Automotive Rail-Sized Carbon Fiber Reinforced Composite Tubes: Part I: Tubes with Woven Reinforcements (Carbon, Kevlar, and Glass) and Non-plug Crush Initiators," presented at the ASC 17th Annual Technical Conference, 10/23/02, West Lafayette, IN, and published as paper No. 46 in the conference CD "*Proceedings of the American Society for Composites 17th Technical Conference*", Oct. 2002.
3. Browne, A. L., Zimmerman, K. B., "Dynamic Axial Crush of Automotive Rail-Sized Carbon Fiber Reinforced Composite Tubes: Part II: Tubes with Braided Reinforcements (Carbon, Kevlar, and Glass) and Non-plug Crush Initiators," presented at the 2002 ASME Mechanical Engineering Congress and Exposition, 11/19/02, New Orleans, LA, and published as paper No. IMECE2002-32949 in the conference CD.
4. Browne, A. L., Iobst, S. and Zimmerman, K. B., "Dynamic Axial Crush of Automotive Rail-Sized Carbon Fiber Reinforced Composite Tubes: Part III: Braided vs. Woven Reinforcements (Carbon, Kevlar, and Glass) and Non-plug Crush Initiators," ICCM-14, San Diego CA, 7/16/03, and published as paper number 0656 in the conference CD.
5. Thornton, P.H., "The Crush Behavior of Pultruded Tubes at High Strain Rates", *Journal of Composite Materials*, Vol. 24, pp. 594-615, 1990.
6. Farley, G.L., "Effect of Fiber and Matrix Maximum Strain on the Energy Absorption of Composite Materials", *Journal of Composite Materials*, Vol. 20, No. 4, pp. 322-334, 1986.
7. Farley, G.L., "Energy Absorption of Composite Materials", *Journal of Composite Materials*, Vol. 17, No. 3, pp. 267-279, 1983.
8. Karbhari, V.M., Falzon, P.J., and Herszberg, I., "Energy Absorption Characteristics of Hybrid Braided Composite Tubes", *Journal of Composite Materials*, Vol. 31, No. 12, pp. 1164-1186, 1997.
9. Chiu, C.H., Tsai, K.-H., and Huang, W.J., "Effects of Braiding Parameters on Energy Absorption Capability of Triaxially Braided Composite Tubes", *Journal of Composite Materials*, Vol. 32, No. 21, pp. 1964-1983, 1998.
10. Hull, D., "A Unified Approach to Progressive Crushing of Fibre-Reinforced Composite Tubes", *Composite Science and Technology*, Vol. 40, pp. 377-421, 1991.
11. Hamada, H., Ramakrishna, S., and Satoh, H., "Effect of Fiber Orientation on the Energy Absorption Capability of Carbon Fiber/PEEK Composite Tubes", *Journal of Composite Materials*, Vol. 30, No. 8, pp. 947-969, 1996.
12. Ramakrishna, S. and Hull, D., "Energy Absorption Capability of Epoxy Composite Tubes With Knitted Carbon Fibre Fabric Reinforcement", *Composites Science and Technology*, Vol. 49, No. 4, pp. 349-356, 1993.
13. Browne, Alan L., and Botkin, Mark E., "Dynamic Axial Crush of Automotive Rail-Sized Composite Tubes Part 4: Plug vs. Non-Plug Crush Initiators," presented at the ASC 19th Annual Technical Conference, 10/21/04, Atlanta, GA, and published as paper no. IE9 in the Conference CD "*Proceedings of the Joint American Society for Composites/American Society for Testing and Materials Committee D30*", Oct. 2004.
14. Farley, G.L., "Effect of Specimen Geometry on the Energy Absorption Capabilities of Composite Materials", *Journal of Composite Materials*, Vol. 20, No. 4, pp. 390-400, 1986.
15. Fairfull, A.H. and Hull, D., "Effects of Specimen Dimensions on the Specific Energy Absorption of Fibre Composite Tubes", *Proceedings of the Sixth International Conference on Composite Materials (ICCM VI) and Second European Conference on Composite Materials (ECCM 2)*, 20-24 July 1987, Vol. 3, pp. 3.36-3.45, 1987.
16. Hamada, H. and Ramakrishna, S., "Scaling Effects in the Energy Absorption of Carbon-Fiber/PEEK Composite Tubes", *Composites Science and Technology*, Vol. 55, No. 3, pp. 211-221, 1995.

17. Mamalis,A.G., Manolakos,D.E., Ioannidis,M.B., and Pappostolou,D.P., "Crashworthy Characteristics of Axially Statically Compressed Thin-Walled Square CFRP Composite Tubes: Experimental", *Composite Structures*, Vol. 63, No. 3-4, pp. 347-360, 2004.
18. Thornton,P.H., "Energy Absorption in Composite Structures", *Journal of Composite Materials*, Vol. 13, pp. 247-262, 1979.
19. Karbhari,V.M. and Haller,J.E., "Rate and Architecture Effects on Progressive Crush of Braided Tubes", *Composite Structures*, Vol. 43, No. 2, pp. 93-108, 1998.
20. Schmueser,D.W. and Wickliffe,L.E., "Impact Energy Absorption of Continuous Fiber Composite Tubes", *Journal of Engineering Materials and Technology*, Transactions of the ASME, Vol. 109, No. 1, pp. 72-77, 1987.
21. Schultz,M.R., Hyer,M.W., and Fuchs,H.P., "Static and Dynamic Energy-Absorption Capacity of Graphite-Epoxy Tubular Specimens", *Mechanics of Composite Materials and Structures*, Vol. 8, No. 3, pp. 231-247, 2001.
22. Browne, Alan L., and Johnson, Nancy L., "Dynamic Crush Tests Using a "Free-Flight" Drop Tower: Theory," *Experimental Techniques*, Vol. 26, No. 5, pp. 43-46, Sept./Oct. 2002.
23. Johnson, Nancy L., and Browne, Alan L., "Dynamic Crush Tests Using a "Free-Flight" Drop Tower: Practical Aspects," *Experimental Techniques*, pp. 47-49, Vol. 26, No. 6, Nov./Dec. 2002.
24. Beard,S.J. and Chang,F.K., "Energy Absorption of Braided Composite Tubes", *International Journal of Crashworthiness*, Vol. 7, No. 2, pp. 191-206, 2002.
25. Kerth,S. and Maier,M., "Numerical Simulation of the Crushing of Composite Tubes", *Proceedings of the 4th International Conference on Computer Aided Design in Composite Material Technology*, Southhampton, UK, June 1994, pp. 141-148, 1994.
26. Caliskan,A.G., "Design & Analysis of Composite Impact Structures for Formula One Using Explicit FEA Techniques", *Proceedings of the 2002 SAE Motorsports Engineering Conference and Exhibition*, Indianapolis, Indiana, 2-5 December, 2002, 2002.
27. Morthorst,M. and Horst,P., "Failure Model for Composite Materials Under Quasi-Static Crushing Conditions", *Journal of Strain Analysis for Engineering Design*, Vol. 39, No. 5, pp. 411-421, 2004.
28. Xiao,X., Johnson,N., and Botkin,M., "Challenges in Composite Tube Crash Simulations", *Proceedings of the American Society for Composites 18th Technical Conference*, ASC 154, Gainesville, FL, USA, 19-22 October 2003, 2003.
29. Williams, K. V., "A Physically-Based Continuum Damage Mechanics Model for Numerical Prediction of Damage Growth", Ph. D. Thesis, The University of British Columbia, 1998.
30. Williams,K.V., Vaziri,R., and Poursartip,A., "A Physically Based Continuum Damage Mechanics Model for Thin Laminated Composite Structures", *International Journal of Solids and Structures*, Vol. 40, pp. 2267-2300, 2003.
31. Floyd, A., "An engineering approach to the simulation of gross damage development in composite laminates", Ph.D. Thesis, Department of Civil Engineering, The University of British Columbia, Vancouver, BC, Canada, 2004.
32. DeTeresa,S.J., Allison,L.M., Cunningham,B.J., Freeman,D.C., Saculla,M.D., Sanchez,R.J., and Winchester,S.W., "Experimental Results in Support of Simulating Progressive Crush in Carbon-Fiber Textile Composites", Vol. UCRL-ID-143287, March 12, 2001, 2001.
33. Sivashanker,S., "Damage Propagation in Multidirectional Composites Subjected to Compressive Loading", *Metallurgical and Materials Transactions A-Physical Metallurgy and Materials Science*, Vol. 32, No. 1, pp. 171-182, 2001.
34. Sivashanker,S., Fleck,N.A., and Sutcliffe,M.P.F., "Microbuckle Propagation in a Unidirectional Carbon Fibre-Epoxy Matrix Composite", *acta materialia*, Vol. 44, No. 7, pp. 2581-2590, 1996.
35. Bazant,Z.P. and Planas,J., "Fracture and Size Effect", 1998.
36. Zobeiry,N., McGregor,C., Vaziri R., and Poursartip A., "A Constitutive Model to Simulate Progressive Compressive Failure in Composites", To be submitted for publication in *Composites A*, 2007.

37. Zobeiry, N., "Progressive Damage Modeling of Composite Materials under Compressive Loads", MSc. Thesis, Department of Civil Engineering, The University of British Columbia, 2005.
38. Xiao, X., "Axial Crash Simulations of Braided Carbon Composite Tubes Using LS-DYNA", Presentation, University of British Columbia, 2003.